RESEARCH ARTICLE

INTERNATIONAL RESEARCH JOURNAL OF MULTIDISCIPLINARY TECHNOVATION

Asian Research Association

DOI: 10.54392/irjmt2659

Experimental Investigation on the Engineering Properties of a Novel Geomaterial Containing Bottom Ash, Blast Furnace Slag and EPS Beads

Akhand Pratap Singh [a, *], R.R.L. Birali [b],

[a] Department of Civil Engineering, Shri Rawatpura Sarkar University, Raipur-492015 (Dist.), Chhattisgarh, India

[b] Department of Civil Engineering, MATS University, Aarang -493441, Raipur (Dist.), Chhattisgarh, India

* Corresponding Author Email: easymade828@gmail.com

DOI: https://doi.org/10.54392/irjmt2659

Received: 12-04-2026; Revised: 23-08-2026; Accepted: 10-09-2026; Published: 15-09-2026

Check for updates

Abstract: This study presents the experimental findings on a Novel Geomaterial (NGM) developed using bottom ash as the primary constituent material. The NGM was made by mixing bottom ash with blast furnace slag and some expanded polystyrene beads, and it relied on ordinary Portland cement as the binder for real. Five different EPS bead contents 0.2%, 0.4%, 0.6%, 0.8% and 1.0% were considered as mix ratios. Blast furnace slag was incorporated at three replacement levels of 4%, 8%, and 12%. In addition, two cement to bottom ash weight ratios, 20% and 30%, were adopted in the study. The experimental program looked at compressive strength, the stress-strain behavior, density, plus the initial tangent modulus for the NGM while using various mix designs and different curing times. The researchers performed compressive strength tests on 70 mm cube samples that were cured for 7 days, 14 days, and 28 days. The results indicate that compressive strength consistently improved with increasing slag content, higher cement dosage, and longer curing duration across all mix ratios, with recorded strengths ranging from 135 kPa to 1020 kPa. The stress–strain behavior exhibited a nonlinear relationship, with compressive stress increasing progressively with axial strain. Furthermore, the density of the prepared NGM decreased from 993 kg/m³ to 611 kg/m³ depending on the mix ratios, while the initial tangent modulus showed a positive correlation with compressive strength. The findings show a kind of manageable trade-off between density and short-term compressive behavior, but the whole thing around environmental sustainability and field readiness is still up in the air, mostly because embodied carbon assessment, leachability checks, durability testing, and wider field-scale validation still need to be done.

Keywords: Novel Geomaterial, Bottom Ash, Blast Furnace Slag, Expanded Polystyrene (EPS) Beads, Mix Ratio, Compressive Strength and Density.

1. Introduction

Indian industries generate a lot of by-products every year, such as coal ash from thermal power plants and blast furnace slag from iron-making factories. When coal is burned, it produces two kinds of ash: fly ash and bottom ash. Fly ash is a fine dust that comes from the smoke released during combustion, and it is collected using electrostatic precipitators to recover it. The furnace bottom releases bottom ash which consists of unburnt coal that has a coarser size than the other ash materials. Coal-based thermal power generation produces fly ash and bottom ash as its principal solid residues. Fly ash consists predominantly of fine particles collected from flue gases, whereas bottom ash is the relatively coarse fraction discharged from the lower part of the furnace. According to the Central Electricity Authority, coal- and lignite-based thermal power stations in India generated approximately 270.82 million tonnes of fly ash during 2021-2022, of which 259.86 million tonnes, corresponding to 95.95%, was reported as utilized. Although the national utilization rate has increased substantially, the large absolute quantity generated annually continues to require technically viable and environmentally responsible utilization pathways. The incorporation of coal combustion residues into engineered fills and construction materials is therefore relevant not only for waste management but also for reducing the consumption of conventional natural materials [1, 2]. Developing countries such as India face difficulties with environmentally safe disposal of their large coal ash quantities because the country has a low land-to-population ratio. The current projects aim to use coal ashes as construction materials for civil engineering projects. Various researchers have carried out studies for the proper utilization of bottom ash, [3-6].

One of the components of the production of blast furnace slag is the separation of iron metal from the slag crust in the iron-smelting process. The whole process involves ore dressing and reduction of iron metal and dross separation. Blast-furnace slag is a non-metallic co-product generated during the reduction of iron ore in a blast furnace and is compositionally and functionally distinct from steelmaking slag. Reliable consolidated statistics for the annual global production and utilization of blast-furnace slag are not available. The U.S. Geological Survey estimates that the quantity of iron slag generated from blast furnaces is generally equivalent to approximately 25-30% of crude pig-iron production. Depending on its cooling history and processing route, blast-furnace slag may be obtained in air-cooled, expanded, or granulated form and can be utilized in cementitious materials, aggregates, ground improvement and other civil-engineering applications [7]. Its incorporation into engineered geomaterials may therefore provide a productive utilization route while modifying the density, grading and mechanical response of the resulting composite [8]. Slag disposal also creates big challenges for the environment. An attempt has been made to use slag in civil engineering applications. Cement clinker production incorporates blast furnace slag as a raw material. When granulated blast furnace slag is mixed with slag-cement and cement by-pass dust, it causes flocculation to form, which helps reduce the soil's tendency to swell [9]. Ground granulated blast furnace slag functions as a material for highway construction and foundation work [10]. The environmental protection from pollution gets enhanced through slag recycling activities. Various researchers have carried out studies for proper utilization of blast furnace slag in engineering applications [11, 12, 14-16].

EPS beads are hydrophobic and non-biodegradable [17, 18]. It prevents absorption of water due to its closed cell structure and has highly compressible property. For back filling of abutments and retaining walls, construction of embankments, EPS beads was used as a lightweight fill material [19]. Research work has investigated Lightweight fill material created from Expanded Polystyrene beads through their combination with bottom ash and fly ash, soil, and stone dust, and binder materials, which included cement [7, 11, 19-24].

Previous studies have established that the engineering response of EPS-based lightweight geomaterials depends strongly on the type of particulate matrix, EPS dosage, binder content and curing regime. Liu *et al.* [19] prepared a soil EPS cement lightweight fill using 2-6% EPS beads and 10-15% cement and reported densities of approximately 700-1100 kg/m³, with the resulting material proposed for irregular filling zones requiring greater strength than conventional EPS blocks. Padade and Mandal [25] investigated a fly ash EPS cement system containing 0.5-2.5% EPS and 10-20% cement, in which the density decreased from approximately 1320 to 725 kg/m³ while the binder dosage controlled the strength and stiffness. Lal and Badwaik [20] subsequently evaluated bottom ash EPS cement mixtures containing 0.3-1.5% EPS and 10% or 20% cement at curing ages of 7, 14 and 28 days; their material achieved a lower density range of 360-650 kg/m³, although strength and initial tangent modulus decreased as EPS content increased. More importantly, a bottom ash–blast-furnace slag EPS cement system has already been reported using 0.9-1.5% EPS, 5-15% slag, a fixed cement ratio of 30%, and curing periods of 14 and 28 days, with compressive strength ranging from 273 to 703 kPa [7, 24, 25]. Recent fly-ash-based research has also considered EPS density, EPS ratio, cement content, curing age and strength-to-density ratio for selecting lightweight and higher-strength filling mixtures [9].

Compared with the previously reported four-component system, the present investigation broadens the experimental design by considering lower EPS contents, two cement levels instead of a single fixed cement dosage, and an additional 7 day curing age. This broader matrix enables the early age and long term effects of EPS, slag and cement contents on density, strength and apparent stiffness to be evaluated within a common experimental framework. Since specimen geometry, curing conditions and testing procedures differ among the reported studies, the comparison is used to identify relative performance trends rather than to claim direct or universal superiority. Against this background, the present investigation does not claim novelty merely from the combination of bottom ash, blast furnace slag, EPS beads and cement. Instead, it extends the previously investigated four-component system towards lower EPS contents of 0.2-1.0%, slag ratios of 4-12%, two cement to bottom-ash ratios of 20% and 30%, and curing periods of 7, 14 and 28 days. Within this experimental range, the material exhibited densities of 611-993 kg/m³, compressive strengths of 135-1020 kPa and apparent initial tangent modulus values of 15–100 MPa.

The present material does not provide an absolute advantage over all previously reported systems, because earlier bottom-ash mixtures achieved lower densities and some fly-ash mixtures attained higher strengths. Its meaningful contribution lies in evaluating the coupled density–strength–stiffness trade-off within the selected four-component design space and identifying mixtures for maximum strength, minimum density and maximum strength-to-density ratio. The recorded terminal axial-strain range of 0.6-2.3% is reported as a deformation characteristic and not as evidence of superior ductility. Accordingly, the material is considered a preliminary candidate for lightweight load-reducing fill, while its suitability for a specific field application remains subject to durability, environmental and field-scale validation.

2. Materials and Methodology

In this study, a sort of fresh geomaterial was made by combining five different ingredients, namely bottom ash, EPS beads, blast furnace slag, ordinary Portland cement, and water. In Table 1, the physical properties of blast furnace slag along with bottom ash are displayed. The work relied on EPS beads that were more or less spherical in form, with a size that varied between 2 and 4 millimeters, and a density of 22 kg per cubic meter. The experimental part also involved ordinary Portland cement of grade 53, as the main cement part (IS 8112, 1989) [3].

2.1. Mix ratios and preparation of the Specimen

The experimental study uses EPS beads and bottom ash to create a mix ratio, which shows their weight relationship through percentage calculation. The calculation of mix ratios is based on previous research [23, 25, 26]. The dry weight of bottom ash (WBA) equals the maximum dry unit weight (γ_{dmax}) multiplied by the dry bottom ash volume (VBA). VBA was evaluated by subtracting the volume of EPS beads (VB) and the volume of blast furnace slag (VS) from the total volume of the cubical specimen (V = 343 cc), that is, VBA = V – VB–VS. The first mix ratio value 0.2 % was achieved by considering VB and VS as 35 cc. The EPS beads weight assessment used the formula WB = ρB × VB where ρB represents EPS beads density. The evaluation of slag percentage WS/WBA was conducted using WBA along with three different slag percentages 4 % 8 % and 12 % that were tested in the experimental program. The researchers established two ratios for the cement weight to bottom ash weight which were 20 % and 30 %. The evaluation of water volume (Vw) was conducted by multiplying WBA with the optimum moisture content (OMC) of bottom ash. Based on this methodology, the remaining mix proportions and corresponding material quantities were systematically determined. The experimental program deployed five mix ratios which are presented in Table 2. Accurate measurement of all materials was carried out with the aid of an electronic weighing balance. Bottom ash, blast furnace slag, and cement were thoroughly blended to create a uniform mass. The compound mixture received water in a gradual process after the initial watering. The addition of EPS beads was completed while the remaining water was added, and the mixing continued until the beads achieved even distribution throughout the mixture. Figure 1 shows the mixing various materials. The prepared mixture was poured into cube moulds and compacted using a tamping rod. After the setting period ended, the team removed the specimens from the moulds and placed them in a water tank for curing.

Table 1. Physical properties of bottom ash, and blast furnace slag

Property	Bottom Ash	Blast Furnace Slag
Specific gravity (G)	1.91	2.2
D_{10} (mm)	0.43	0.6
D_{30} (mm)	0.6	0.8
D_{60} (mm)	1.1	1.0
Uniformity coefficient (C_u)	2.56	1.67
Coefficient of curvature (C_c)	0.761	1.07
Dry unit weight (kN/m^3)	13.9	14
Optimum moisture content (OMC) (%)	30	10

Table 2. Different mix proportions used in the experimental program

Mix Ratio $\left(\frac{WB}{WBA}\right)\times100$	Slag $\left(\frac{WS}{WBA}\right)\times100$	Cement $\left(\frac{WC}{WBA}\right)\times100$
0.2	4 %, 8 %, 12 %	20 %, 30 %
0.4	4 %, 8 %, 12 %	20 %, 30 %
0.6	4 %, 8 %, 12 %	20 %, 30 %
0.8	4 %, 8 %, 12 %	20 %, 30 %
1.0	4 %, 8 %, 12 %	20 %, 30 %

Figure 1. Photograph of mixing of different material.

2.1.1 Model Calculation and Weights of Materials for Mix Ratio of 0.2%

Weight of Beads WB =0.77 grams

Weight of Bottom Ash WBA = 387 grams

Weight of Slag WS for 4% = 15.5 grams; 8%=31 grams; 12%= 46.5 grams

Weight of Cement WC for 20%= 77.4 grams; 30%= 116.1 grams

Volume of Water VW=116 ml

For other mix ratios mentioned or given in table 2, the weights of the materials are calculated accordingly.

The constituent materials were weighed using an electronic weighing balance. Bottom ash, blast-furnace slag, and cement were initially dry-mixed until a uniform mixture was obtained. A portion of the calculated water was then added gradually. The density of the NGM decreased with increasing EPS mix ratio across all tested WS/WBA and WC/WBA ratios. The specimen density decreased from 903 kg/m³ to 611 kg/m³ with an increase in EPS content from 0.2% to 1.0% at a WC/WBA ratio of 20%, while it decreased from 993 kg/m³ to 639 kg/m³ at a WC/WBA ratio of 30%. The EPS beads used in the study had a density of 22 kg/m³ and were highly compressible. The initial tangent modulus of the NGM decreased with increasing mix ratio, while higher stiffness was observed with higher compressive strength. The initial tangent modulus values ranged from 15 to 100 MPa. The prepared mixture was placed in 70 × 70 × 70 mm cube moulds and compacted using a tamping rod. After the initial setting period, the specimens were demoulded and transferred to a water-curing tank for the specified curing duration.

2.2. Experimental Procedure

The testing procedure used in this present study is similar to that reported by [20, 26] and [19, 27]. First, the specimens were taken out from the curing process and their weight was checked for air-dry testing. Then the team tested the NGM specimens under a controlled deformation rate of 0.12 mm per minute, to get their compressive strength by using a compression testing machine. This machine was used on specimens sized 70 x 70 x 70 mm. In order to follow the vertical movement and also the compression force, they linked a load cell with a linear variable differential transducer (LVDT) together to make the measurements. Before everything was connected to the data logger, the testing equipment was prepared by calibrating both the load cell and the LVDT first, then installing them.

The specimens were water-cured for 7, 14, and 28 days before testing. Compressive strength was determined from the maximum load recorded during the compression test. The experimental program consisted of five mix ratios, three WS/WBA ratios, two WC/WBA ratios, and three curing periods. Three specimens were prepared and tested for each selected mix proportion, resulting in a total of 270 tested specimens. One specimen from each mix ratio and curing period was additionally tested to assess reproducibility. The test results showed good repeatability, with deviation ranging from 3% to 6%.

The initial tangent modulus was used to represent the relationship between stress and strain at the beginning of loading. The initial tangent modulus values obtained for the NGM ranged from 15 to 100 MPa.

3. Results and Discussion

3.1. Density

NGM density depends on its parameters, which include the slag percentages, cement percentages, and mix ratio values affected. The density of NGM decreases with higher mix ratios across all different WS/WBA and WC/WBA ratios. The density measurements at different mix ratios show how they affect the density of NGM according to Figure 2. The NGM prepared using WS/WBA ratio of 12 % has shown highest value of density compared to WS/WBA ratio of 4 % and 8 % for all mix and WC/WBA ratio. The density of NGM decreased as the WS/WBA percentages decreased. The measured density of the NGM ranged from 611 to 993 kg/m³. Although a substantial portion of these values lies within the range of 700-1100 kg/m³ reported by Liu *et al.* [19], the minimum-density mixtures fall below that interval. In particular, the specimen containing 1.0% mix ratio, 4% WS/WBA and 20% WC/WBA exhibited the lowest density of 611 kg/m³ and a corresponding 28-day compressive strength of approximately 277.2 kPa. This result indicates that increasing the EPS content can produce a greater reduction in self-weight than previously reported materials, although this advantage is accompanied by a reduction in compressive strength. Therefore, the low-density mixtures should be evaluated on the basis of their combined density and load-carrying capacity rather than density alone [20, 21].

The reduction in density with increasing EPS content is primarily associated with the replacement of a portion of the relatively dense cemented ash matrix by EPS beads having a density of only 22 kg/m³. As the EPS ratio increases, the volume occupied by lightweight inclusions increases while the proportion of the load-bearing mineral skeleton decreases. Any voids formed around the beads during mixing and compaction may further reduce the bulk density; however, such interfacial voids were not directly quantified in the present study. Conversely, increasing the cement and slag contents increases the proportion of solid mineral constituents and therefore produces a comparatively denser composite. Similar reductions in density with increasing EPS content have been reported for bottom ash, fly-ash and soil based EPS geomaterials [20, 21, 25].

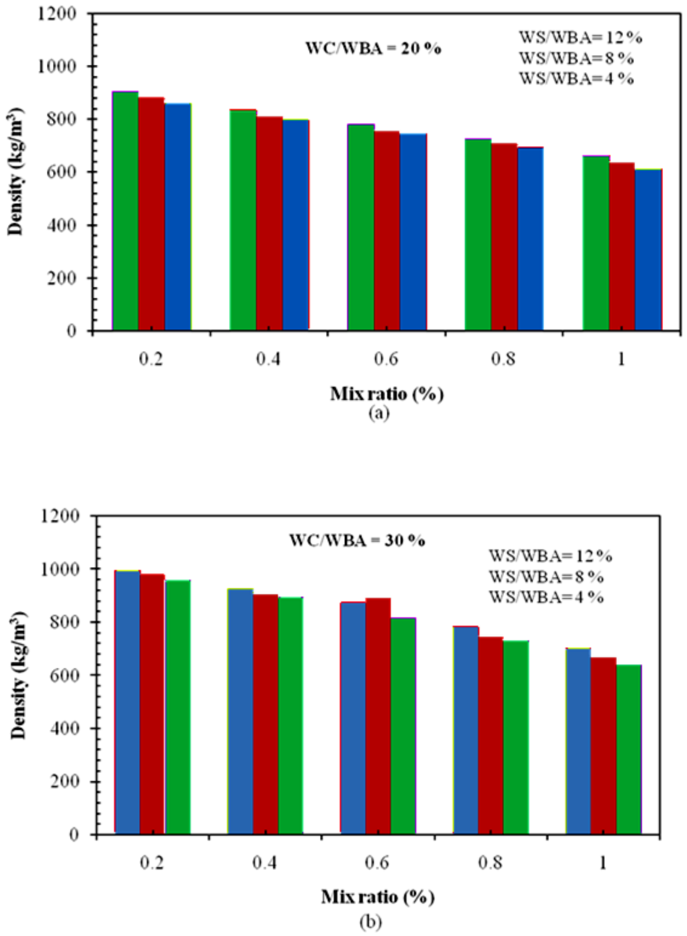

Figure 2. Effect of mix ratios on density of NGM for (a) WC/WBA = 20 %, (b) WC/WBA = 30 %.

3.2 Failure Pattern

When an axial compressive load was applied, the failure patterns of NGM got observed. In other words, all the specimens ended up failing within an axial strain range of about 0.6% to 2.3%, so it was quite consistent. Before the final failure, every specimen developed vertical cracks that seemed to start from the top part of the specimen, then those same cracks went on downward, all the way to the bottom. The overall failure pattern for the NGM specimen is presented in Figure 3.

3.3 Compressive Strength

The effect of different amounts of slag and cement, along with various mix ratios and curing times, was studied to understand how they affect the compressive strength of the NGM samples. The highest stress value reached during testing is referred to as compressive strength. The results in Figure 4 show how different mix ratios affected the compressive strength results for all WS/WBA ratios and curing periods which used 20% WC/WBA mixture. Throughout all curing times and different WS/WBA ratios, there was a clear connection between the mix proportion and the compressive strength. Figure 5 shows the Relationship between compressive strength and mix ratios for all the WS/WBA percentages and curing period days, when WC/WBA = 30 % (a) 7 days, (b) 14 days and (c) 28 days. At both WC/WBA ratios, the compressive strength decreased with an increase in mix ratio from 0.2% to 1.0% for all slag level and curing ages. For each combination of WS/WBA and WC/WBA ratios, the highest compressive strength was achieved at a 0.2% mix ratio, while a 1.0% mix ratio resulted in the lowest compressive strength. Under compression, the incorporation of EPS beads affects the compressive strength and stiffness of the NGM. EPS beads are highly compressible, and increasing the EPS mix ratios from 0.2% to 1.0% resulted in a consistent reduction in compressive strength across the tested WS/WBA and WC/WBA ratios and curing periods. The stiffness of the NGM also decreased with increasing mix ratio, while higher stiffness was associated with higher compressive strength. These results indicate that increasing the EPS content leads to reductions in both compressive strength and stiffness of the NGM. The observed behavior is consistent with the use of EPS beads as lightweight inclusions in bottom-ash-based geomaterials reported in previous studies [20, 21, 25].

The increase in compressive strength when cement content went up, and curing age as well, was seen across all the tested mix ratios. The results show that when the cement dosage is higher, and the curing period lasts longer, the NGM ends up with a higher compressive strength. Also, the compressive strength of the NGM went higher as the slag content increased across the tested WC/WBA ratios and over different curing periods. The specimens cured for 28 days showed a higher compressive strength compared to the ones cured for 7 and 14 days.

Figure 3. Failure pattern of Novel Geomaterial (NGM) specimen.

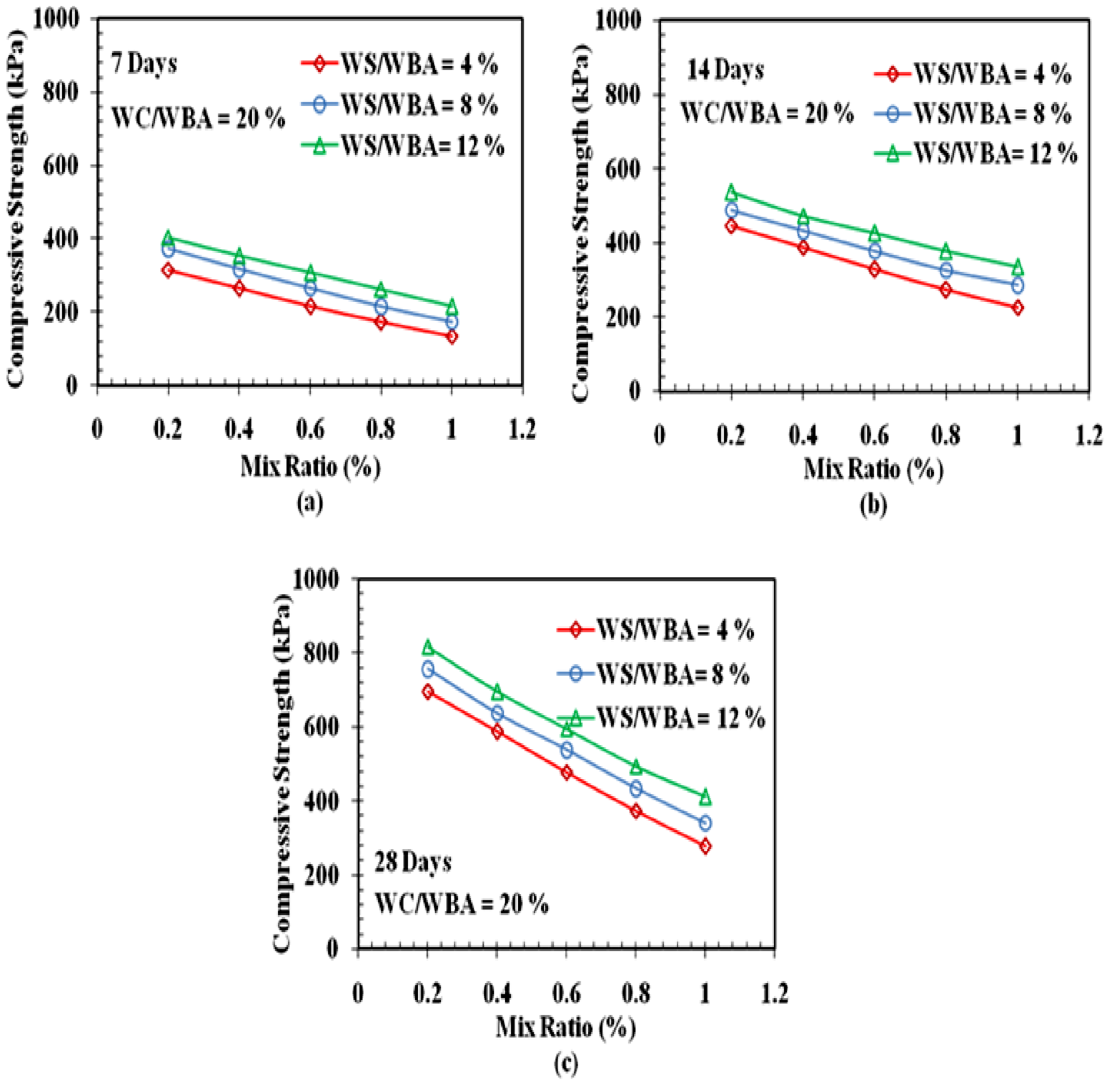

Figure 4. Relationship between compressive strength and mix ratios for all the WS/WBA percentages and curing period days, when WC/WBA = 20 % (a) 7 days, (b) 14 days and (c) 28 days.

The NGM prepared with 12% WS/WBA ratio showed better compressive strength results than the NGM made with 4% and 8% WS/WBA ratios at both WC/WBA ratios throughout all curing periods. Figure 6 shows how compressive strength develops in relation to WS/WBA values during all curing periods at a WC/WBA ratio of 20 percent. The same behavior was observed again when the WC/WBA ratio was 30%. The 28 day cured NGM specimen had the highest compressive strength among all mix ratios at various WS/WBA and WC/WBA levels. The researchers noticed that both WC/WBA ratios showed a clear link between the WS/WBA value and compressive strength. The study showed that all mix ratios had increasing compressive strength values, which were directly connected to higher WS/WBA values across all curing periods.

The increase in compressive strength observed at higher WS/WBA ratios is supported by the experimental results. The NGM prepared with a 12% WS/WBA ratio showed higher compressive strength than those prepared with 4% and 8% WS/WBA ratios at both WC/WBA ratios throughout all curing periods. The results showed that compressive strength increased with increasing WS/WBA values across all curing periods. The NGM with a WS/WBA ratio of 12% also showed better stiffness performance compared with the specimens prepared with 4% and 8% WS/WBA ratios, regardless of the mix ratio or curing period.

Table 3 and Table 4 show the compressive strength results for all the mix ratios, WS/WBA percentages, and curing periods that are relevant to both WC/WBA ratios. The 28-day compressive strength for each mix ratio was higher than the values recorded at 7 and 14 days. As the curing period increased, the compressive strength values decreased with higher mix ratio levels. NGM displays compressive strength values between 135 kPa and 1020 kPa. The study shows that present research found higher compressive strength values than the lightweight fill material range of 100 to 510 kPa established by Liu et al. [19] and the geomaterial range of 150 to 686 kPa reported by Ram Rathan Lal and Badwaik [20].

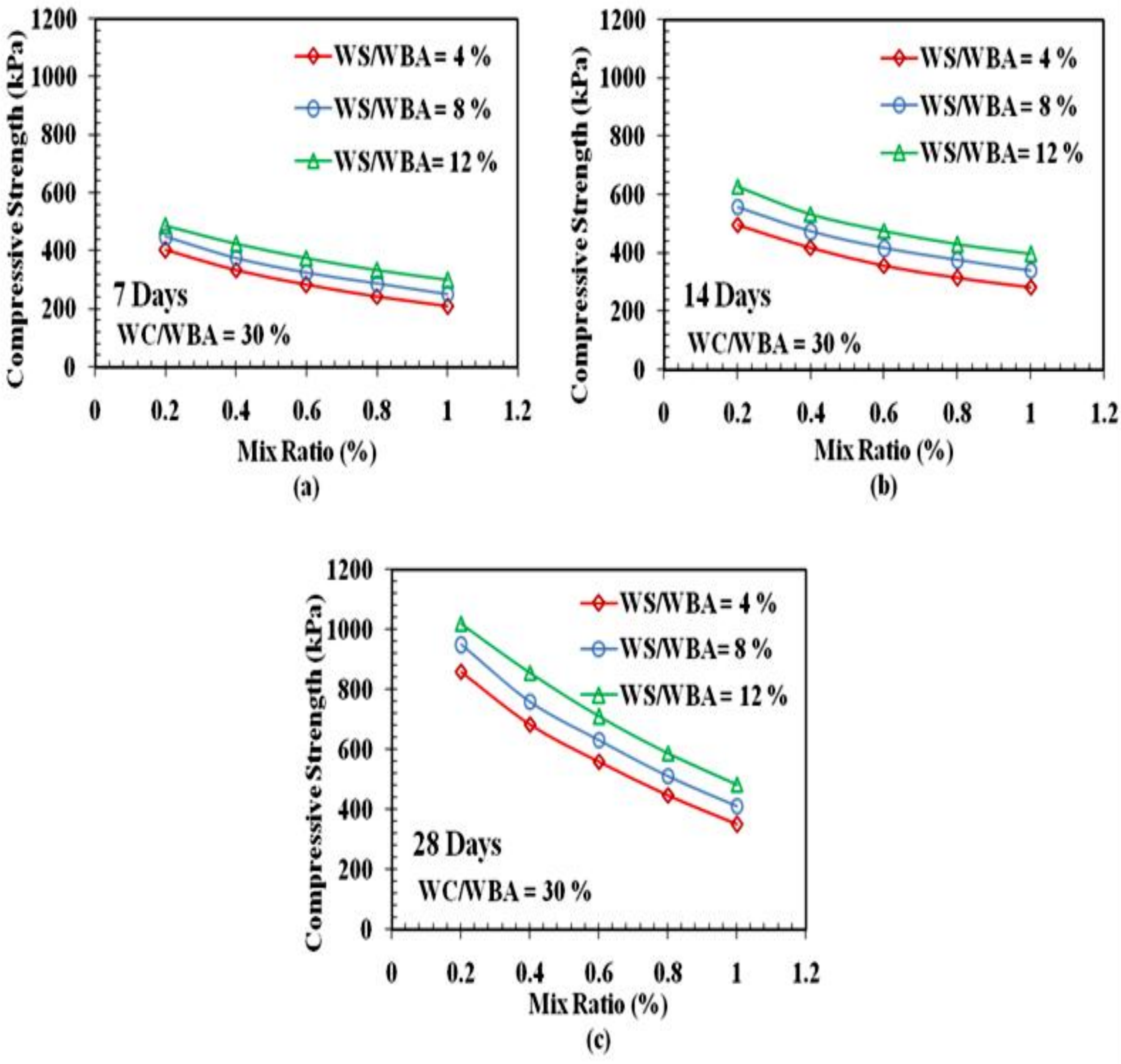

Figure 5. Relationship between compressive strength and mix ratios for all the WS/WBA percentages and curing period days, when WC/WBA = 30 % **(a)** 7 days, **(b)** 14 days and **(c)** 28 days.

Table 3. Compressive strength of bottom ash based material for WC/WBA=20 %

Mix ratio (%)	Compressive strength (kPa)								
	7 Days			14 Days			28 Days		
	WS/WBA (%)			WS/WBA (%)			WS/WBA (%)		
	4	8	12	4	8	12	4	8	12
0.2	315.204	372.755	404.358	446.939	489.184	536.735	697.224	757.837	817.633
0.4	264.429	317.041	353.571	388.163	432.041	473.265	588.245	638.041	695.388
0.6	215.408	266.429	307.592	328.714	378.449	425.388	477.837	537.837	595.184
0.8	172.347	214.592	263.163	273.469	326.735	377.959	373.347	434.367	493.755
1.0	135.245	173.98	215.408	226.735	285.714	335.51	277.224	341.714	410.898

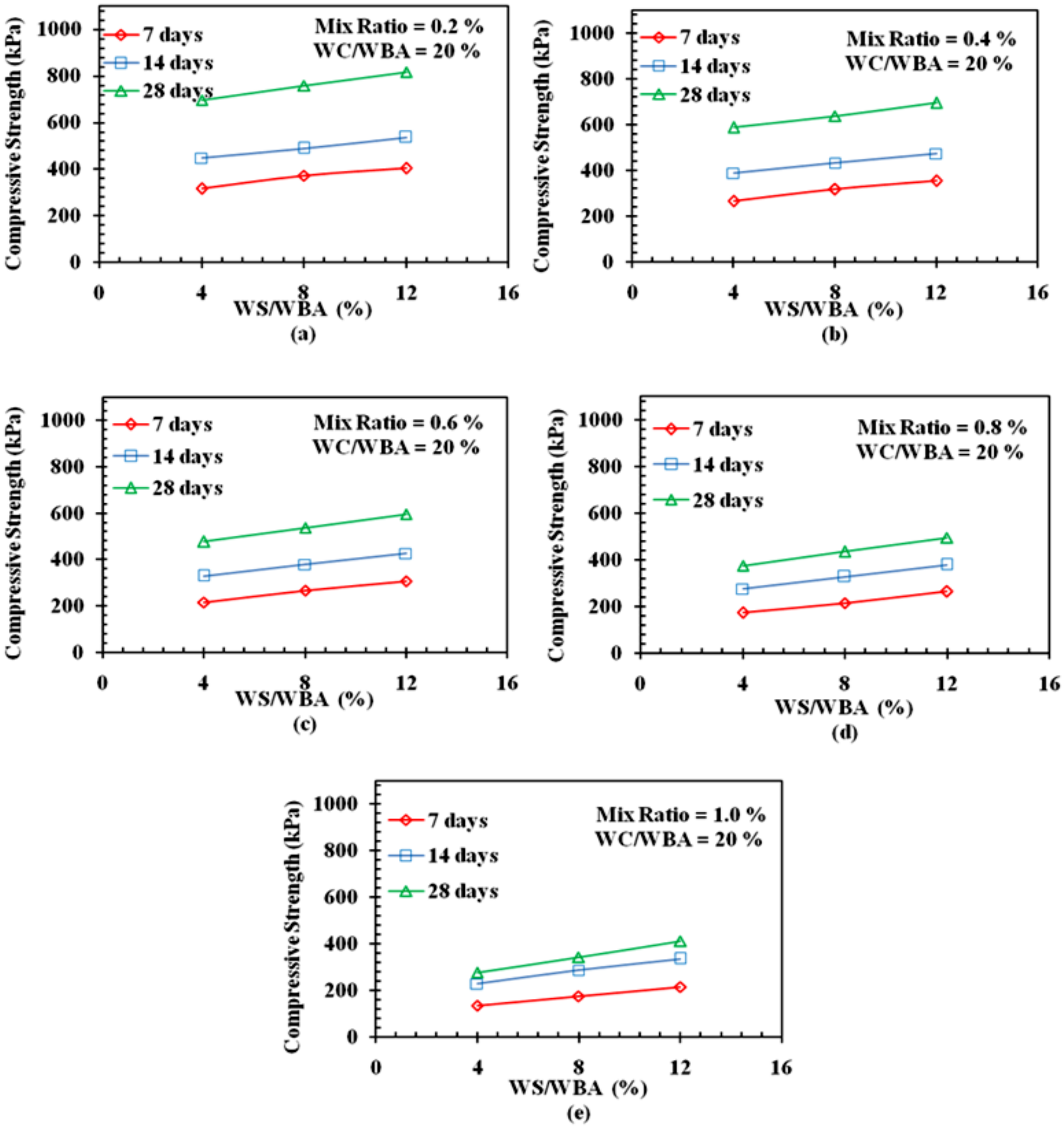

Figure 6. Relationship between compressive strength and different WS/WBA ratios with WC/WBA ratio 20 % for all the curing period days and mix ratios **(a)** 0.2 %, **(b)** 0.4 %, **(c)** 0.6 %, **(d)** 0.8 % and **(e)** 1.0 %.

Table 4. Compressive strength of bottom ash based material for WC/WBA = 30 %

Mix ratio (%)	Compressive strength (kPa)								
	7 Days			14 Days			28 Days		
	WS/WBA (%)			WS/WBA (%)			WS/WBA (%)		
	4	8	12	4	8	12	4	8	12
0.2	403.163	449.082	486.020	496.939	559.184	627.551	860.082	949.878	1020.082
0.4	335.408	377.857	424.388	419.388	473.673	534.082	683.959	760.490	855.592
0.6	284.796	326.837	376.633	357.143	416.735	475.571	560.490	632.939	709.061
0.8	245.612	288.265	334.388	313.469	376.735	428.980	448.245	512.735	588.857
1.0	208.469	252.755	301.327	283.469	341.429	395.714	350.286	411.510	483.143

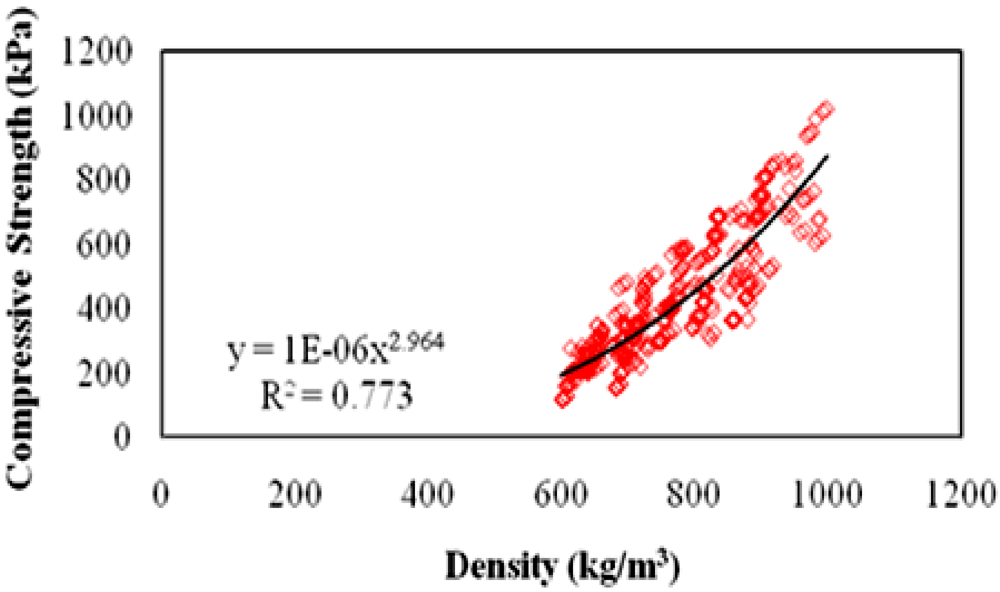

Figure 7. Relationship between compressive strength and density values for all WS/WBA ratios.

Figure 7 illustrates how all the WS/WBA and WC/WBA ratios in NGM relate compressive strength to density. The relationship between compressive strength (σ) and density (ρ) fits well with a power equation, which can be expressed as

$$\sigma = 1E\text{-}06\rho^{2.964}$$

Where, σ is in kPa and ρ is in kg/m^3

The increase in compressive strength with increasing WS/WBA ratio cannot be attributed exclusively to the independent cementitious activity of blast-furnace slag because the experimental matrix did not include a zero-slag control mixture. Moreover, the cement contents of 20% and 30% relative to bottom-ash mass are sufficiently high to contribute substantially to matrix bonding and curing-related strength development. Under the present conditions, the slag may have acted as a granular replacement that increased the solid fraction and improved particle packing, as a denser inclusion that reduced internal void space, or potentially as a partially reactive supplementary constituent. However, the relative contributions of these mechanisms cannot be separated without chemical characterization and control mixtures containing bottom ash and cement without slag. Therefore, the reported effect of slag is limited to the observed increase in strength associated with higher WS/WBA ratios and should not be interpreted as proof of an independent slag-reaction mechanism.

The cement dosages used in the present study are relatively high for large-volume embankment or backfill applications. Consequently, the preferred mixtures identified here represent mechanical performance optima within the tested design space rather than cost- or sustainability-optimized field formulations.

3.4. Stress - Strain Pattern

Utilizing the data from compressive strength tests to determine both stiffness properties and stress-strain characteristics of the NGM material. The mix ratio values had an impact on the WS/WBA ratios, resulting in different compressive stress and axial strain curves for all WS/WBA ratios throughout the 28th day curing period. This is shown in Figure 8 for the WC/WBA 20% mix and Figure 9 for the WC/WBA 30% mix. The results from the 7th and 14th day curing periods showed similar trends for both WC/WBA ratios. The researchers observed that the stiffness of the NGM increased with longer curing times and higher WS/WBA ratios across all mix and WC/WBA ratio combinations. The NGM made with a WS/WBA ratio of 12% performed better in terms of stiffness compared to the NGM made with WS/WBA ratios of 4% and 8%, regardless of the mix ratio or curing period. The NGM stiffness decreased with every mix ratio increase throughout the curing time. The 28th day cured NGM specimen exhibited maximum stiffness across all mix ratios. The WS/WBA percentage determined the NGM stress-strain behavior and its compressive strength. All NGM mixtures exhibited a nonlinear stress–strain response comprising an ascending branch, a distinct peak stress and subsequent post-peak softening. However, no standardized ductility index was evaluated during the present experimental programme. The peak axial strain, defined as the strain corresponding to the maximum compressive stress, was determined for each specimen. The compressive stress relationship with axial strain exhibited non-linear behavior across all mix ratios and WC/WBA ratios.NGM specimens exhibited their failure pattern when subjected to compressive load testing. The specimens experienced complete failure through all testing procedures which extended from 0.6 % to 2.3 % axial strain.

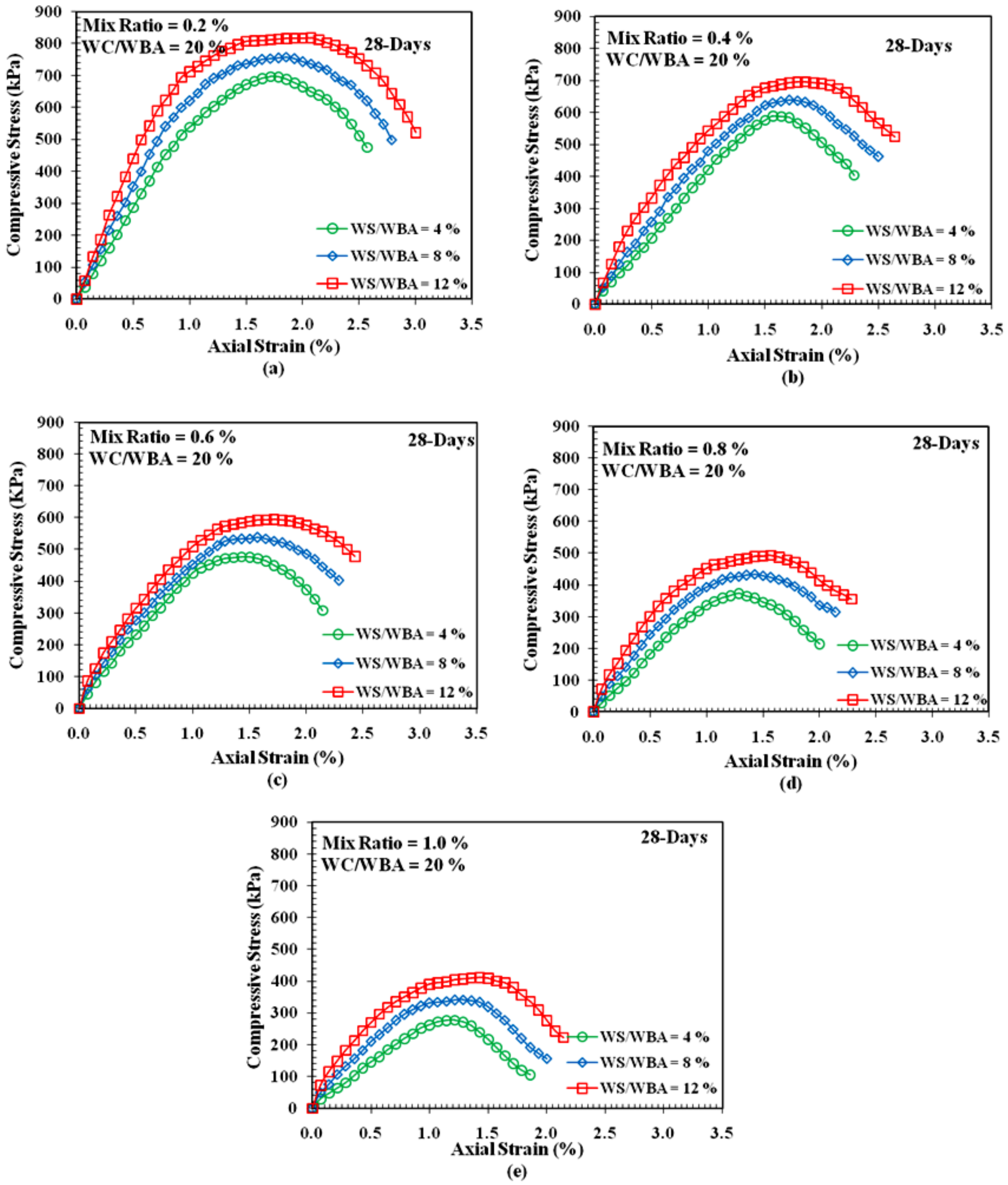

Figure 8. Compressive stress and axial strain curves, over the 28-day curing period, with a WC/WBA ratio of 20%, for every WS/WBA ratio and mix ratio, namely (a) 0.2 %, (b) 0.4 %, (c) 0.6 %, (d) 0.8%, and (e) 1.0.

The specimens exhibited vertical cracks that started from their uppermost point before they reached their breaking point. The vertical cracks ran all the way from the top of the specimen down to its bottom edge. The compressive stress–strain relationship of the NGM exhibited nonlinear behavior across all mix ratios and WC/WBA ratios. The NGM specimens experienced complete failure during compressive loading, with failure occurring at axial strain values ranging from 0.6% to 2.3%. Vertical cracks were observed in the specimens before reaching the breaking point, extending from the top of the specimen to the bottom edge. The stiffness of the NGM decreased with every increase in mix ratio, while higher stiffness was observed with longer curing times and higher WS/WBA ratios. The NGM specimens prepared with a WS/WBA ratio of 12% exhibited better stiffness performance than those prepared with 4% and 8% WS/WBA ratios, regardless of the mix ratio or curing period. [26].

3.5. Apparent Initial Tangent Modulus

The modulus values reported in this study represent the initial stiffness obtained from platendisplacement measurements and therefore include possible contributions from seating and machine compliance. The relationship between stress and strain at the start of loading is usually captured by that initial tangent modulus (Ei), you know, the initial bit. In general, higher Ei numbers tend to show up in materials with higher compressive strength, which is kind of intuitive. The Ei values are commonly around the 15 to 100 MPa range, give or take, so they're not exactly all over the place. The connection between the initial tangent modulus (Ei) and compressive strength (σ) is shown in Figure 10.

The current study's findings show that the initial tangent modulus values are higher than those reported by Ram Rathan Lal and Badwaik [20] for geomaterials (14-40 MPa) and higher than those reported by Horvath [18], Stark et al. [28], and Padade and Mandal [29] for EPS geofoam blocks, which normally range from 2.2 to 11.4 MPa. However, according to Liu et al. [19], the obtained values are lower than those of lightweight fill materials, which vary from 79 to 555 MPa. Table 5 lists the Comparison of EPS beads-based material with NGM of Present Study.

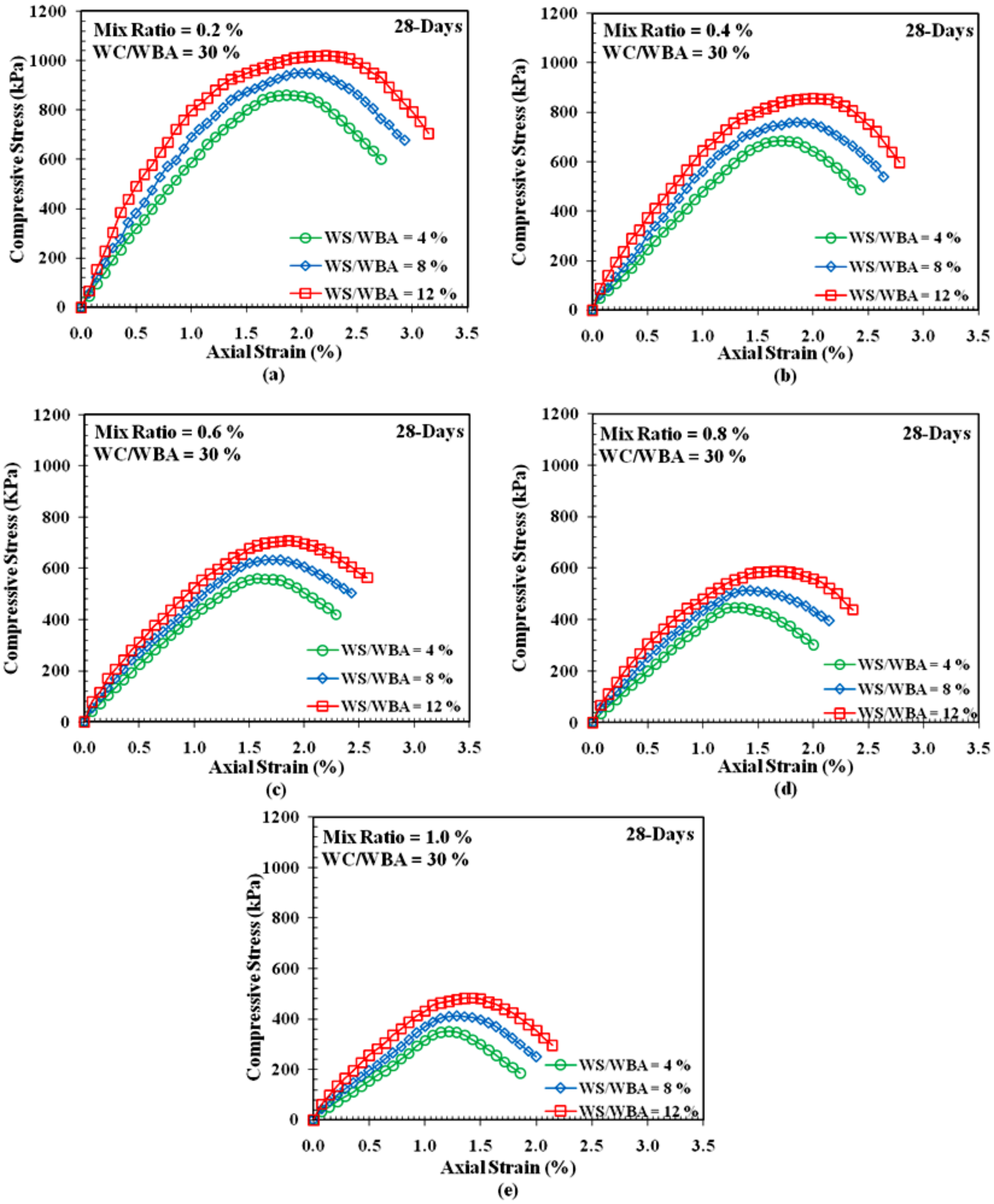

Figure 9. Compressive stress and axial strain curves over the 28-day curing period, with the WC/WBA ratio at 30% for every one of the WS/WBA ratios plus the mix ratios (a) 0.2%, (b) 0.4%, (c) 0.6%, (d) 0.8% and (e) 1.0%.

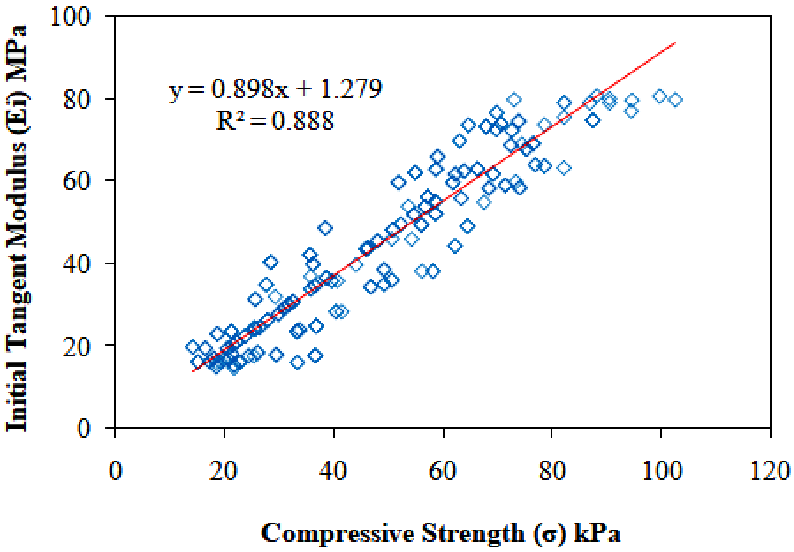

Figure 10. Correlation between initial tangent modulus and compressive strength for Novel Geo Material (NGM), with all the WS/WBA and the WC/WBA ratios as well.

Table 5. Comparison of EPS beads-based material with NGM of Present Study

	Material	Density (kg/m^3)	Compressive Strength (kPa)	Initial Tangent Modulus (MPa)
Liu et al. [19]	Lightweight fill material	700–1100	100–510	79–555
Padade and Mandal [25]	EPGM	725-1320	355-3290	51-500
Ram Rathan Lal and Badwaik [20]	Geomaterial	360-650	150-686	14-40
Ram Rathan Lal and Nawkhare [30]	Lightweight fill material	500-800	38-294	6-45
Marjive et al. [22]	EPS–Stone dust	960-2010	236-515	12-85
Pande and Padade [7]	FAGM	831-1341	750-7800	93-589
Present Study	NGM	611-993	135-1020	15-100

The formula shows a linear kinda relationship between the compressive strength (σ) and the initial tangent modulus (Ei).

$$E_i = 0.898\sigma + 1.279$$

Where σ = compressive strength of the NGM, (kPa); and Ei= initial tangential modulus (MPa).

3.6 Performance-Based Mixture Selection and Preliminary Application Assessment

The preferred mixture depends on the intended engineering performance rather than on a single material property. The specimen containing 0.2% mix ratio, 12% WS/WBA and 30% WC/WBA, cured for 28 days, achieved the maximum compressive strength of approximately 1020 kPa at a density of 993 kg/m³. This mixture also exhibited the highest strength to density index of approximately 1.027 kPa/(kg/m³), indicating the most favourable load carrying capacity relative to self weight among the tested formulations. In contrast, the specimen containing 1.0% mix ratio, 4% WS/WBA and 20% WC/WBA produced the minimum density of 611 kg/m³, with a corresponding 28th day compressive strength of approximately 277 kPa. Thus, the former mixture is preferable where load capacity governs the design, whereas the latter is more suitable where maximum reduction in self-weight is required and moderate strength is acceptable.

Increasing cement and slag contents was not considered uniformly beneficial because the associated strength gain was accompanied by increased density, apparent stiffness, material consumption and potential environmental burden. The 0.2% mix ratio, 12% slag, 30% cement mixture provided the maximum strength of 1020 kPa, but it also had the highest density of 993 kg/m³ and the greatest cement demand. Conversely, the 1.0% mix ratio, 4% slag, 20% cement mixture achieved the minimum density of 611 kg/m³, but its 28th day strength decreased to approximately 277 kPa, and the higher EPS content may increase sensitivity to mixing uniformity and segregation. As a screening-level multi-criteria compromise, the specimen containing 0.4% mix ratio, 8% slag and 20% cement, cured for 28 days, was identified as the preferred balanced formulation. It achieved a compressive strength of approximately 638 kPa at a density of about 810 kg/m³, corresponding to a strength to density index of approximately 0.79 and a cement-use efficiency of 31.9 kPa per percentage point of cement. The use of an intermediate EPS and slag content provides substantial self-weight reduction while avoiding the highest cement dosage and the maximum EPS content. However, this selection remains preliminary because material cost, mixing energy, flowability, compaction effort, segregation and field placement were not measured directly.

Based on the measured properties, the present NGM is considered primarily as a preliminary lightweight load-reducing fill for confined, nonstructural backfill zones where reduction of overburden pressure is the principal design objective. Its density range of 611-993 kg/m³ corresponds to a unit weight of approximately 6.0-9.7 kN/m³. This range is comparable to the 600-1040 kg/m³ range reported by the Federal Highway Administration for expanded shale and clay lightweight fills and is substantially below the reference range of 1522-2403 kg/m³ for conventional mineral soils and aggregates. Thus, depending on the selected mixture and reference fill, the material may reduce fill self-weight by approximately 35-75% [27]. The measured 28 day compressive-strength range of approximately 0.277-1.020 MPa also overlaps the 0.3-2.1 MPa range commonly reported for low-strength cemented backfill materials. ACI 229R indicates that strengths of approximately 0.3-0.7 MPa may provide bearing capacity comparable to well-compacted fill. However, the present NGM was placed by tamping rather than as a self-consolidating mixture, and its flowability was not evaluated; therefore, it is not classified as controlled low-strength material. Moreover, permeability, drainage capacity, shear strength, compressibility, creep, cyclic response, saturation resistance and long-term durability were not investigated. Consequently, the present results support only preliminary consideration as a lightweight load-reducing fill and do not establish compliance for retaining-wall backfill, embankment cores, utility trenches or other field applications.

This present study, it was kind of limited to laboratory compression tests carried out on NGM specimens cured for 7, 14, and 28 days. The measured compressive strength and the initial tangent modulus, they are meant to reflect the mechanical behaviour of the NGM under the specific testing conditions that were used here. So the obtained results, they mainly apply to the tested mixtures as well as the curing conditions. For the rest, further investigations are still necessary in order to assess how the NGM will actually perform in real field conditions.

In the present study, the water-related performance was not really evaluated, so the impacts of bottom ash and blast-furnace slag on hydraulic behaviour were also not looked into. The density that was reported, together with compressive strength and the initial tangent modulus, match the laboratory conditions used here. That said, additional work is still needed, because the hydraulic performance of the NGM should be reassessed before any real field application.

4. Conclusions

This study established the short-term unconfined compressive response of a bottom-ash-based lightweight geomaterial incorporating blast-furnace slag, EPS beads and cement over a defined compositional and curing range. The principal demonstrated contribution is the systematic identification of the density, strength, stiffness trade-off produced by varying EPS, slag and cement contents. Within the investigated mixtures, density ranged from 611 to 993 kg/m³, compressive strength from 135 to 1020 kPa, and apparent initial tangent modulus from 15 to 100 MPa.

The measured trends indicate that increasing EPS content reduces density but also decreases strength and apparent stiffness because the low-density, highly compressible beads replace part of the cemented mineral skeleton and reduce the effective load-bearing solid fraction. Increasing cement content and curing age improves strength through progressive development of cementitious bonding within the ash–slag matrix. The higher strength observed with increasing slag content may additionally reflect increased solid fraction and improved particle packing. The material is most appropriately considered as a preliminary lightweight load-reducing fill for confined, nonstructural backfill zones where reduction of self-weight is a primary requirement. The 0.2% mix ratio, 12% slag, 30% cement mixture cured for 28 days provided the maximum strength of approximately 1020 kPa but also produced the highest density and cement demand. The 1.0% mix ratio, 4% slag, 20% cement mixture achieved the minimum density of 611 kg/m³ but provided comparatively low 28-day strength of approximately 277 kPa. Considering lightweight performance, load capacity, cement consumption and likely mixing practicality, the 0.4% mix ratio, 8% slag, 20% cement mixture cured for 28 days is proposed as the preliminary balanced formulation. This selection should be confirmed using its verified mixture-specific density, stiffness, cost and field-constructability data.

The conclusions are valid only for the tested constituent sources, mix ratios of 0.2-1.0%, slag ratios of 4-12%, cement-to-bottom-ash ratios of 20% and 30%, curing periods of 7-28 days, and short-term laterally unconfined compression of 70 mm cube specimens. The measured compressive strength and apparent tangent modulus should therefore be treated as laboratory screening parameters rather than direct field-design properties. Confinement-dependent shear strength, compressibility, creep, cyclic response, stress-dependent stiffness, permeability, water absorption, saturation resistance, wet–dry durability and long-term strength retention remain to be established.

The use of bottom ash and slag demonstrates substantial industrial-by-product incorporation, but it does not independently establish environmental sustainability because of the relatively high cement demand, non-biodegradable EPS and absence of embodied-carbon and leachability assessments. Accordingly, recommendations for sustainable infrastructure, predictive design or field-scale implementation should remain conditional until durability, environmental safety and full-scale performance have been experimentally validated.

Abbreviations

EPS	Expanded Polystyrene
NGM	Novel Geomaterial
IS	Indian Standard
LVDT	Linear Variable Differential Transducer
OMC	Optimum Moisture Content

Annotations

E_i	Initial tangent modulus
VBA	Volume of bottom ash
V	Total volume of specimen
VB	Volume of EPS beads
VS	Volume of blast furnace slag
Vw	Volume of water
WBA	Dry weight of bottom ash
WB	Weight of beads
γ_{dmax}	Maximum dry unit weight of bottom ash
ρ_B	Density of EPS beads
σ	Compressive Strength

References

[1] D. Kumar, N. Kumar, A. Gupta, Geotechnical properties of fly and bottom ash mixtures in different proportions. International Journal of Science and Research, 3(9), (2014) 1487–1494. https://www.ijsr.net/getabstract.php?paperid=SEP14444

[2] Z.T. Yao, M.S. Xia, P.K. Sarker, T.Z. Chen, A review of the alumina recovery from coal fly ash, with a focus in China. Fuel, 120, (2014) 74–85. https://doi.org/10.1016/j.fuel.2013.12.003

[3] Bureau of Indian Standards, IS 8112. (1989). Specification for 43 Grade Ordinary Portland cement. New Delhi, India.

[4] B. Kim, M. Prezzi, R. Salgado, Geotechnical properties of fly and bottom ash mixtures for use in highway embankments. Journal of Geotechnical and Geoenvironmental Engineering, 131(7), (2005) 914–924. https://doi.org/10.1061/(ASCE)1090-0241(2005)131:7(914)

[5] B.L. Phillips, J. Groppo, R. Perrone, Evaluation of processed bottom ash for use as lightweight aggregate in the production of concrete masonry units. In Proceedings World of Coal Ash (WOCA), (2005) 1–10.

[6] M.S.H.M. Sani, F.B. Muftah, Z. Muda, The properties of special concrete using washed bottom ash (WBA) as partial sand replacement. International Journal of Sustainable Construction Engineering and Technology, 1(2), (2010) 65–76. https://journal.uthm.edu.my/index.php/IJSCET/article/view/64

[7] A.Y. Pande, A.H. Padade, Engineering performance of lightweight geomaterial influenced by EPS density and mix ratio. Emerging Materials Research, 12(4), (2023) 358–371. https://doi.org/10.1680/jemmr.23.00041

[8] P.E. Tsakiridis, G.D. Papadimitriou, S. Tsivilis, C. Koroneos, Utilization of steel slag for Portland cement clinker production. Journal of Hazardous Materials, 152(2), (2008) 805–811. https://doi.org/10.1016/j.jhazmat.2007.07.093

[9] A. Al-Rawas, Microfabric and mineralogical studies on the stabilization of an expansive soil using cement by-pass dust and some types of slags. Canadian Geotechnical Journal, 39(5), (2002) 1150–1167. https://doi.org/10.1139/t02-046

[10] S. Wild, J.M. Kinuthia, G.M. Jones, D.D. Higgins, Effects of partial substitution of lime with ground granulated blast furnace slag (GGBS) on the strength properties of lime-stabilized sulphate-bearing clay soils. Engineering Geology, 51(1), (1998) 37–53. https://doi.org/10.1016/S0013-7952(98)00039-8

[11] D. Mandal, B. Ram Rathan Lal, Compressive and Flexural Behaviour of Glass Fibre Reinforced Blast Furnace Slag Based Material. In: Reddy, K.R., Agnihotri, A.K., Yukselen-Aksoy, Y., Dubey, B.K., Bansal, A. (eds) Sustainable Environment and Infrastructure. Lecture Notes in Civil Engineering, Springer, Cham, 90, (2021) 147-156. https://doi.org/10.1007/978-3-030-51354-2_14

[12] H.R. Nikhade, B. Ram Rathan Lal, Studies on sugarcane bagasse ash and blast furnace slag based geomaterial. In Proceedings IGGEC 2021, Lecture Notes in Civil Engineering, 280, (2022) 25–32. https://doi.org/10.1061/9780784480472.091

[13] H.R. Nikhade, B. Ram Rathan Lal, Effect of addition of glass fibers on sugar cane bagasse ash under compressive loading. Materials Today: Proceedings, 61(3), (2022) 1109–1114. https://doi.org/10.1016/j.matpr.2021.11.063

[14] H.R. Nikhade, B. Ram Rathan Lal, K. Ansari, M.A. Khan, H.M. Najm, S.M. Anas, M. Mursaleen, M.A. Hasan, S. Islam, Behaviour of geomaterial composite using sugar cane bagasse ash under compressive and flexural loading. Frontiers in Materials, 10, (2023) 1108717. https://doi.org/10.3389/fmats.2023.1108717

[15] D. Mandal, B. Ram Rathan Lal, K. Shanker. (2018). Compressive strength behaviour of glass fibre reinforced blast furnace slag-based material. In Proceedings of the 11th International Conference on Geosynthetics (ICG 2018).

[16] D. Mandal, B. Ram Rathan Lal. (2019). Compressive load behavior of glass fiber reinforced blast furnace slag-based material. In Proceedings National Conference on Sustainable Infrastructure Development and Management (SIDM-97). https://dx.doi.org/10.2139/ssrn.3380074

[17] J.S. Horvath, Expanded polystyrene geofoam: An introduction to material behaviour. Geotextiles and Geomembranes, 13(4), (1994) 263–280. https://doi.org/10.1016/0266-1144(94)90048-5

[18] J.S. Horvath, The compressible-inclusion functions of EPS geofoam: Analysis and design methodologies. Geotextiles and Geomembranes, 15(1-3), (1997) 77–120. https://doi.org/10.1016/S0266-1144(97)00008-3

[19] H.L. Liu, A. Deng, J. Chu, Effect of different mixing ratios of polystyrene pre-puff beads and cement on the mechanical behaviour of lightweight fills. Geotextiles and Geomembranes, 24, (2006) 331–338. https://doi.org/10.1016/j.geotexmem.2006.05.002

[20] B. Ram Rathan Lal, V.N. Badwaik, Experimental studies on bottom ash and expanded polystyrene beads-based geomaterial. Journal of Hazardous, Toxic, and Radioactive Waste, 20(2), (2015) 04015020. https://doi.org/10.1061/(ASCE)HZ.2153-5515.0000305

[21] D. Mandal, B. Ram Rathan Lal, Compressive and Flexural Behaviour of Glass Fibre Reinforced Blast Furnace Slag Based Material. In: Reddy, K.R., Agnihotri, A.K., Yukselen-Aksoy, Y., Dubey, B.K., Bansal, A. (eds) Sustainable Environment and Infrastructure. Lecture Notes in Civil Engineering, Springer, Cham, 90, (2021) 147-156. https://doi.org/10.1007/978-3-030-51354-2_14

[22] V.R. Marjive, B. Ram Rathan Lal, An experimental study on stone dust and EPS beads based material. In GeoChicago 2016: Sustainability, Energy and the Geoenvironment, (2016) pp. 33–41.

[23] V.R. Marjive, B. Ram Rathan Lal, (2016) Compressive strength behaviour of stone dust and EPS beads-based material. In Geotechnical and Structural Engineering Congress. https://doi.org/10.1061/9780784480151.004

[24] A.Y. Pande, A.H. Padade, Engineering potential of pond ash geomaterial: A lightweight filling solution. International Journal of Geomechanics, 24(8), (2024) 04024175. https://doi.org/10.1061/IJGNAI.GMENG-8388

[25] A.H. Padade, J.N. Mandal, Expanded polystyrene-based geomaterial with fly ash. International Journal of Geomechanics, 14(6), (2014) 06014013. https://doi.org/10.1061/(ASCE)GM.1943-5622.0000390

[26] B. Ram Rathan Lal, S.S. Nawkhare, Experimental study on plastic strips and EPS beads reinforced bottom ash based geomaterial. International Journal of Geosynthetics and Ground Engineering, 2(3), (2016) 25. https://doi.org/10.1007/s40891-016-0066-2

[27] I. Qamhia, E. Tutumluer, J. Nicks, M. Adams, M. Khan, Lightweight and alternative backfills for highway applications: State-of-the-art practice in the U.S.A. Transportation Research Record: Journal of the Transportation Research Board, 2678(5), (2024) 677–688. https://doi.org/10.1177/03611981231191519

[28] T.D. Stark, D. Arellano, J.S. Horvath, D. Leshchinsky, (2004). Geofoam Application in Design and Construction of Highway Embankments, NCHRP Web Document 65. Washington, DC, USA: Transportation Research Board.

[29] A.H. Padade, J.N. Mandal, Feasibility studies on expanded polystyrene (EPS) geofoam. In Proceedings International Conference on Ground Improvement and Ground Technique (IGCI-2012), 2, (2012) 903–976.

[30] S.S. Nawkhare, B.R.R. Lal, Experimental studies on reinforced bottom ash based geomaterial. In Geotechnical Frontiers 2017, 280, (2017) 852–861. https://doi.org/10.1061/9780784480472.091

Acknowledgement

This research was supported by Shri Rawatpura Sarkar University. The authors are thankful to the Director, Shri Rawatpura Sarkar University, Raipur, for granting permission to carry out experimental work at the Raipur research lab.

Authors Contribution Statement

Both the Authors equally contributed, Read and Approved the Final Version of the Manuscript.

Funding

The authors declare that no funds, grants or any other support were received during the preparation of this manuscript.

Competing Interests

The authors state that they do not have any known competing financial interests or personal relationships that might have affected the work that is reported in this paper. On behalf of all authors, the corresponding writer says that there isn't any conflict of interest.

Data Availability

The datasets that were generated, and then analysed in this study, can be obtained from the corresponding author with a reasonable request, if needed.

Has this article screened for similarity?

Yes